J. Plasma Physics (2006), *vol.* 72, *part* 6, *pp.* 799–804.
doi:10.1017/S0022377806004909 Printed in the United Kingdom

Multi-scale modeling of hydrogen isotope transport in porous graphite

M. WARRIER[1], R. SCHNEIDER,[2] E. SALONEN[3] and K. NORDLUND[4]

[1]Institute for Plasma Research, BHAT, Gandhinagar, Gujarat 382428, India

[2]Max-Planck-Institut für Plasmaphysik, D-17491 Greifswald, Germany

[3]Laboratory of Physics and Helsinki Institute of Physics, P.O. Box 1100, FIN-02015 HUT, Finland

[4]Accelerator Laboratory, P.O. Box 43, FIN-00014, University of Helsinki, Finland

(Received 11 August 2005 and accepted 7 November 2005)

Abstract. We describe a general multi-scale method to model hydrogen isotope transport, over length scales from angstroms to centimeters and time scales from picoseconds to several seconds, in a complex three-dimensional porous geometry using molecular dynamics, kinetic Monte Carlo and Monte Carlo diffusion simulations. We present comparisons with experimental results for hydrogen diffusion and hydrogen atom desorption from graphite. Finally, we demonstrate the flexibility of the computational tools used to tackle problems at different scales.

1. Introduction

It is important to understand hydrogen isotope transport in graphite in order to understand and evaluate the continued use of graphite as a first wall and divertor target material in fusion devices. The graphites used as plasma facing materials in fusion devices are porous and consist of granules, a few micrometers in size, separated by voids which are typically a fraction of a micrometer in size. These granules further consist of randomly oriented crystallites, a few nanometers in size, separated by micro-voids which are a few angstroms in size (Fig. 1) [1–4].

The incident hydrogen isotopes from the plasma undergo collisions with the target atoms, create damage and thermalize with the target atoms. There exists a wide variety of interaction possibilities between the thermalized hydrogen isotopes and the substructures of graphite: inter-crystallite diffusion; trans-granular diffusion (TGD); on the internal void–granule interface (VGI), transport can occur by surface diffusion, adsorption–desorption and trapping–detrapping [1, 2, 4]. In order to understand how these microscopic processes affect the macroscopic transport and inventory of hydrogen isotopes, a multi-scale approach, both in space and in time, is required. In this paper we present a multi-scale scheme for hydrogen transport in three-dimensional porous graphite (Sec. 2). The model is applied (Sec. 3) to study hydrogen atom desorption and diffusion in porous graphite and defect agglomeration in bombarded crystal graphite. Finally, conclusions are presented (Sec. 4).

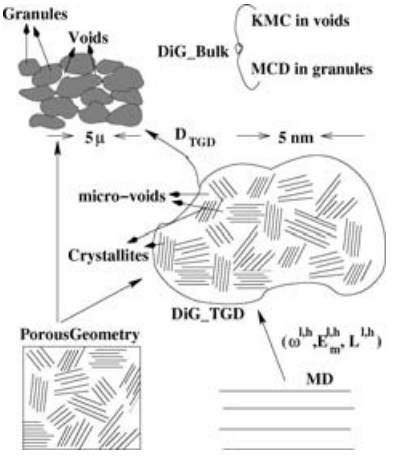

Figure 1. Multi-scale schematic: PorousGeometry is used to create both granules separated by voids and crystallites separated by micro voids; MD is used to study hydrogen transport in crystallites; DiG_TGD handles TGD and DiG_Bulk handles bulk diffusion; various parameters (explained in the text) are transferred from MD to DiG_TGD and from DiG_TGD to DiG_Bulk.

2. Multi-scale simulation scheme

We have developed a multi-scale scheme wherein different computer simulation tools are used at different scales (Fig. 1). Statistical analysis of detailed simulations at lower scales yields the average behavior, which is then used for simulation at the larger scales. Experimental results are used wherever available. The porous geometry of a specified void/microvoid fraction and sub-structure (granules/crystallites) sizes are created using a Poisson distribution for the sub-structure size. For a given volume the sub-structures can be given an irregular shape with required smoothness, and random orientations are assigned by specifying the Euler angles for the rotational transformation.

2.1. Simulation at microscopic scales

At the microscopic scales, molecular dynamics (MD), using the Brenner potential [5] with Nordlund's extension [6], is used to simulate hydrogen isotope diffusion in crystalline graphite. We take 960 carbon atoms at the graphite crystal locations and use Berendsen's pressure and temperature control [7] schemes within the MD code to create zero pressure, sample graphite crystallites between 150 and 900 K using periodic boundary conditions (PBCs). MD simulations of a single hydrogen isotope introduced between the graphene layers were carried out for 100 ps, at the above temperatures.

It is seen that the interstitial does not diffuse across the graphene layer. The isotope trajectories are parametrized as a sum of two trapping–detrapping processes with characteristic jump attempt frequencies ($\omega_o^{\mathrm{l,h}}$), migration energies ($E_{\mathrm{m}}^{\mathrm{l,h}}$) and jump lengths ($L^{\mathrm{l,h}}$); superscripts l and h indicate the low and high migration energy channels. Details of the analysis and results are presented in [8, 9]. It is seen that ω_o^{h} is independent of the isotope mass and ω_o^{l} varies as the inverse square root of the isotope mass.

https://doi.org/10.1017/S0022377806004909 Published online by Cambridge University Press

Based on the theory of dynamical Monte Carlo simulations [10], a time is assigned to a trapping–detrapping kind of random walk for hydrogen trajectories in crystal graphite. Using this and the Bortz–Kalos–Lebowitz (BKL) algorithm [11], to assign transition (jump) probabilities, a kinetic Monte Carlo (KMC) code (DiG) was implemented to scale up in time, length and number of particles. Using the results of the MD simulation as inputs to the KMC code, we are able to reproduce the MD results [9].

2.2. Simulations at the mesoscales

At the mesoscales, a porous granule structure is generated. The MD results at microscales are used in DiG to simulate transport in randomly oriented crystallites. The transport in microvoids is modeled by specifying a trapping probability for the interstitial as it passes through the microvoid–crystallite interface (MCI). Detrapping at the MCI is handled as an additional transition in DiG. The detrapped atoms take a random three-dimensional step. If this step takes it into a microvoid, the interstitial continues its flight until it comes in contact with a MCI where it again has a probability of getting trapped. If the step takes it into a crystallite, it then diffuses in the crystallite.

Simulations were done between 750 and 1750 K. PBCs are applied in the three directions. The trapping probability at the MCI was taken to be 1. The trapping energies $E_t = 2.6$–4.3 eV [12] and detrap attempt frequency $\omega_o^t = 10^{13}\,s^{-1}$ corresponding to the phonon frequency in graphite [2] were used. Details and results of these simulations are presented in [9]. It is seen that the diffusion is isotropic and the crystallite diffusion coefficients are much higher than the the TGD diffusion coefficients (D_{TGD}) due to the low values of E_m^h and E_m^l compared with E_t. The diffusion coefficients obtained lie within the experimental range and it is seen that the void size of the graphite is important and not the void fraction [9]. Assuming isotropic diffusion within the granules, and jump sizes corresponding to voids and crystallite sizes, an analytical expression for the TGD coefficient could also reproduce the experimental results [12].

2.3. Simulations at the macroscales

At the macroscales, the atoms at the VGI and voids are transported using KMC, which also provides the time step (Δt) for the simulation. A Monte Carlo diffusion (MCD) algorithm [13] is used for TGD within the granules. D_{TGD}, obtained from the mesoscopic simulations, is used as input to the MCD algorithm. In MCD, a diffusion can be represented as a random walk of the N particles with the jump size given by $\Delta r = \sqrt{2D\,\Delta t}\zeta$, where D is the diffusion coefficient and ζ is sampled from a random number distribution satisfying $\langle\zeta\rangle = 0$ and $\langle\zeta^2\rangle = 1$.

A cubic granular structure of side length 5×10^{-5} m with an average granule size of 2.5×10^{-6} m and a void fraction of 10% was created. The resolution of the structure was 5×10^{-7} m. PBCs are applied along the X and Y directions, which lie parallel to the graphite surface. Along Z, which lies perpendicular to the graphite surface, the structure is replicated for $Z > 0$. The thermalized hydrogen atom positions are initialized to have a uniform distribution along X–Y and a Gaussian distribution with a specified standard deviation, centered at a depth R, along Z. At the VGI, the energy for detrapping is 2.7 eV, for desorption is 1.91 eV [14] and for surface diffusion is 0.9 eV [15]. The jump attempt frequency assumed is again $10^{13}\,s^{-1}$, which fixes the jump length for surface diffusion at 34.64 Ångstroms.

https://doi.org/10.1017/S0022377806004909 Published online by Cambridge University Press

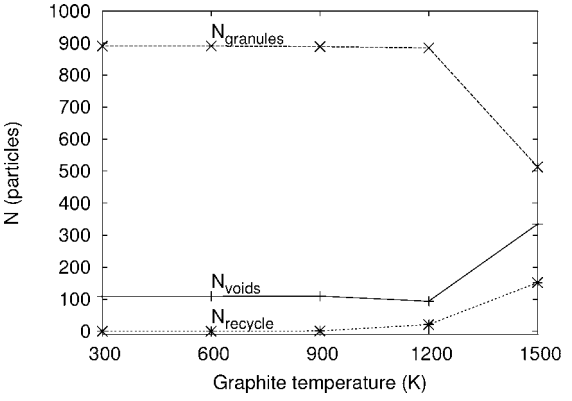

Figure 2. Number of particles in different regions.

Activation energy for entering the surface for a solute hydrogen atom is same as the activation energy for TGD. The simulations are carried out at 300, 600, 900, 1200 and 1500 K.

3. Applications of the multi-scale simulation

The above macroscale simulations are used to study hydrogen atomic desorption and transport in porous graphite. The microscale KMC code was modified to simulate defect agglomeration in irradiated graphite crystals.

3.1. Hydrogen desorption and transport in graphite results

We see that the transport in granules is generally much slower than the transport in the voids and VGI. It is only at high graphite temperatures ($\geqslant$1200 K) that TGD shows up. The number of particles (N) in different regions (subscript) are plotted as a function of target temperature (Fig. 2). Below 900 K there is no transfer of particles from one region to another because the activation energies for bulk diffusion are too high. Most of the transport is by surface diffusion of the solute atoms. Note that desorption of hydrogen atoms from the surface starts off somewhere between 900 and 1200 K as is observed in experiments [15, 16].

The diffusion coefficients obtained from the simulations are plotted in Fig. 3 (labelled DiG) and compared with the surface diffusion expression obtained from experiments [15] (labelled Causey). We see that there exists two different channels for diffusion from the presence of two different slopes seen in Fig. 3. This is because the diffusion is dominated by surface diffusion and adsorption–desorption mechanisms at the VGI. The surface diffusion mechanism leads to the presence of hydrogen atoms deep in open pore graphites (typically a micrometers in a few days at 300 K). We see that fully closed pore graphites prevents this contribution to hydrogen isotope inventory because there is no continuous surface leading deep into the graphite. The difference in the values of the surface diffusion coefficient obtained from our simulation and [15] is because we use granule sizes which are a quarter of the size of those in [15], due to RAM limitations. It must be also mentioned that the method of evaluating the diffusion coefficient ($D = \lim_{t\to\infty}(1/2dt)[r(t)-r(0)]^2$, where the dimensionality $d = 3$ and $[r(t) - r(0)]^2$ is the mean variance in position of the N particles simulated) is naive. Special techniques must be used to interpret diffusion on rough fractal surfaces [17].

https://doi.org/10.1017/S0022377806004909 Published online by Cambridge University Press

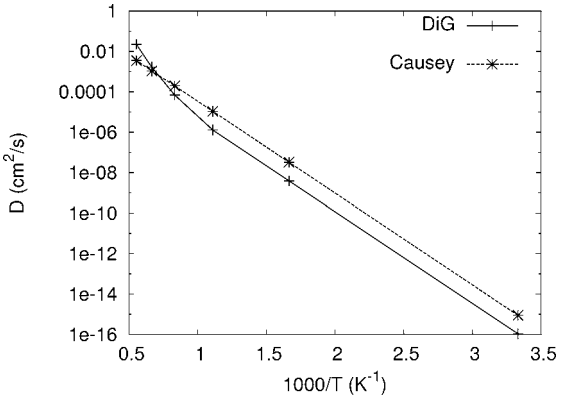

Figure 3. Diffusion coefficient for hydrogen in porous graphite.

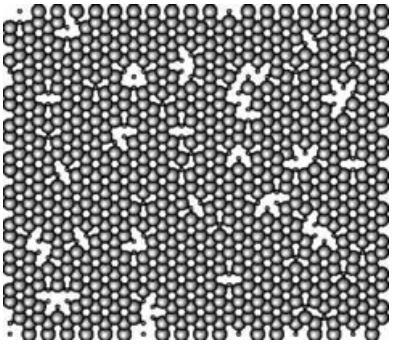

Figure 4. Defect agglomeration observed from our simulations.

3.2. Defect agglomeration in irradiated graphite

It is known that irradiation leads to self-organized phenomena [18]. Scanning tunelling microscopy (STM) analysis of hydrogen irradiation on pure crystalline graphite show defect agglomeration as the incident fluence increases [19]. We use the KMC code at microscales to simulate this phenomena. Vacancies are introduced in pure crystalline graphite with a uniform probability to simulate the defects caused by incident ions. For diffusion of atoms on the graphene layer (and thereby the vacancies) we consider two processes: (i) singly bonded carbon atoms have a higher probability of jumping as compared with doubly bonded carbon atoms; and (ii) atoms within a certain radius of incident ion have a enhanced probability of displacing due to local heating at the point of incidence. The target temperature is taken into account when specifying the probabilities of the various jumps. These two processes are sufficient to reproduce the star-like patterns observed in experiments (Fig. 4). The above model ignores the fact that the vacancy in graphite is not simply that obtained by removing an atom [20] and the effect on the STM images due to buckling of the graphite surfaces due to interstitials between the uppermost graphite layers [21]. These effects can be incorporated in our codes and are part of future work.

https://doi.org/10.1017/S0022377806004909 Published online by Cambridge University Press

4. Conclusion

A general multi-scale scheme to simulate hydrogen transport in porous graphite has been developed. The model reproduces experimental results for hydrogen atom diffusion and desorption in graphites. The flexibility of the codes developed is shown by comparison with experiments at different scales.

References

[1] Möller, W. 1989 Hydrogen trapping and transport in carbon. *J. Nucl. Mater.* **162–164**, 138–150.

[2] Haasz, A. A. *et al.* 1995 Two-region model for hydrogen trapping in and release from graphite. *J. Appl. Phys.* **77**(1), 66–86.

[3] Hassanein, A., Wiechers, B. and Konkashbaev, I. 1998 Tritium behaviour in eroded dust of plasma-facing materials. *J. Nucl. Mater.* **258–263**, 295–300.

[4] Federici, G. and Wu, C. H. 1992 Modeling of plasma hydrogen isotope behaviour in porous materials. *J. Nucl. Mater.* **186**, 131–152.

[5] Brenner, D. W. 1990 Empirical potential for hydrocarbons for use in simulating chemical vapour deposition of diamond films. *Phys. Rev. B* **42**, 9458.

[6] Nordlund, K., Keinonen, J. and Mattila, T. 1996 Formation of ion irradiation induced small-scale defects on graphite. *Phys. Rev. Lett.* **77**, 699.

[7] Berendsen, H. J. C. *et al.* 1984 Molecular dynamics with coupling to an external bath. *J. Chem. Phys.* **81**(8), 3684–3690.

[8] Warrier, M., Schneider, R., Salonen, E. and Nordlund, K. 2004 Modeling of the diffusion of hydrogen in porous graphite. *Physica Scripta*, **T108**, 85.

[9] Warrier, M., Schneider, R., Salonen, E. and Nordlund, K. 2004 Multi-scale modeling of H diffusion in graphite. *Contrib. Plasma Phys.* **44**(1–3), 307–310.

[10] Fichthorn, K. A. and Weinberg, W. H. 1991 Theoritical foundations of dynamical Monte Carlo simulations. *J. Chem. Phys.* **95**(2), 1090–1096.

[11] Bortz, A. B., Kalos, M. H. and Lebowitz, J. L. 1975 A new algorithm for monte carlo simulation of ising spin systems. *J. Comp. Phys.* **17**, 10.

[12] Wilson, K. L. *et al.* 1991 Trapping, detrapping and release of implanted hydrogen isotopes. Atomic and plasma-material interaction data for fusion. (Suppl.) *Nucl. Fusion* **1**, 31–50.

[13] Kloeden, P. E. and Platen, E. 1999 In: *Numerical Solution of Stochastic Differential Equations*. *Appl. Math.*, Vol. 23. Berlin: Springer.

[14] Ashida, K., Ichimura, K., Matsuyama, M. and Watanabe, K. 1984 Thermal desorption of hydrogen, deuterium and tritium from pyrolytic graphite. *J. Nucl. Mater.* **128–129**, 792.

[15] Causey, R. A., Baskes, M. I. and Wilson, K. L. 1986 The retention of D and T in poco axf-5q graphite. *J. Vacuum Sci. Technol. A* **4**(3), 1189–1192.

[16] Franzen, P. and Vietzke, E. 1994 Atomic release of hydrogen from pure and boronized graphites. *J. Vacuum Sci. Technol. A* **12**(3), 820–825.

[17] Havlin, S. and Ben-Avraham, D. 2002 Diffusion in disordered media. *Adv. Phys.* **51**(1), 187–292.

[18] Banhart, F. 1999 Irradiation effects in carbon nanostructures. *Rep. Prog. Phys.* **62**, 1181–1221.

[19] Angot, T. 2004 *Personal communication*, Université de Provence, Marseille.

[20] El-Barbary, A. A., Telling, R. H., Ewels, C. P., Heggie, M. I. and Briddon, P. R. 2003 Structure and energetics of the vacancy in graphite. *Phys. Rev. B* **68**, 144107.

[21] Krasheninnikov, A. V. and Elesin, V. F. 2000 The effect of interstitial clusters and vacancies on the scanning tunneling microscopy image of graphite. *Surface Sci.* **454–456**, 519–524.